BAYESIAN COMPRESSED SENSING IN ULTRASOUND IMAGING

Céline Quinsac[(1)], *Nicolas Dobigeon*[(2)], *Adrian Basarab*[(1)], *Denis Kouamé*[(1)] *and Jean-Yves Tourneret*[(2)]

[(1)]University of Toulouse, IRIT, Toulouse, France
[(2)]University of Toulouse, IRIT/INP-ENSEEIHT/TéSA, Toulouse, France
{celine.quinsac, nicolas.dobigeon, adrian.basarab, denis.kouame, jean-yves.tourneret}@irit.fr

ABSTRACT

Following our previous study on compressed sensing for ultrasound imaging, this paper proposes to exploit the image sparsity in the frequency domain within a Bayesian approach. A Bernoulli-Gaussian prior is assigned to the Fourier transform of the ultrasound image in order to enforce sparsity and to reconstruct the image via Bayesian compressed sensing. In addition, the Bayesian approach allows the image sparsity level in the spectral domain to be estimated, a significant parameter in the ℓ_1 constrained minimization problem related to compressed sensing. Results obtained with a simulated ultrasound image and an *in vivo* image of a human thyroid gland show a reconstruction performance similar to a classical compressed sensing algorithm from half of spatial samples while estimating the sparsity level during reconstruction.

Index Terms— Compressed sensing, ultrasound imaging, Bayesian reconstruction, sparsity.

1. INTRODUCTION

Because it can be implemented easily in real time, ultrasound imaging (UI) has became one of the most popular imaging modalities. However, the volume of data acquired during an examination can limit real time implementations and lead to storage issues. Compressed sensing (CS) is based on the idea of sampling a signal directly into its compressed form [1]. CS has been widely used in various medical imaging domains [2]. Its applicability in UI has been recently shown in [3]. Bayesian approaches have been showing interesting results in reconstructing sparse signals obtained from observations similar to those of CS, i.e., by using random linear combinations of the signal. These methods naturally exploit the intrinsic sparsity of the signals to be reconstructed by defining appropriate priors [4, 5]. The aim of this paper is to present a Bayesian reconstruction method for compressively sensed ultrasound images based on a Bernoulli Gaussian prior for the image Fourier transform. Taking into account the statistic properties of ultrasound images [6] and defining priors promoting sparsity in the frequency domain, we propose a very promising Bayesian algorithm for ultrasound image reconstruction. Reconstructions obtained by this algorithm show normalized root mean squared errors (NRMSEs) similar to those of classical CS up to half of missing pixels. However, the advantage of the proposed method compared to classical CS techniques is that it is completely automatic and does not require to adjust parameters or hyperparameters. In addition, it allows the sparsity level of the image in the frequency domain to be estimated. Such a data reduction could be of large interest in UI, as it could lead to an increase of the acquisition frame rate, which is an issue in number of applications, especially in 3D UI [3].

2. COMPRESSED SENSING IN ULTRASONOGRAPHY

CS consists of estimating a sparse signal $\mathbf{x}$ from a noisy observation vector $\mathbf{y}$, from projections on a complex $M \times N$ random matrix $\mathbf{T}$

$$\mathbf{y} = \mathbf{T}\mathbf{x} + \boldsymbol{\eta} \tag{1}$$

where $\mathbf{y} = (y_1, ..., y_M)^T \in \mathbb{C}^M$ is the measurement vector, $\mathbf{x} = (x_1, ..., x_N)^T \in \mathbb{C}^N$ is the unknown parameter vector and $\boldsymbol{\eta} = (\eta_1, ..., \eta_M)^T \in \mathbb{C}^M$ is an additive complex noise including instrumentation errors and errors due to the signal being only approximately sparse. The estimation of $\mathbf{x}$ can be performed in a deterministic way via a functional minimization penalized by an ℓ_1 criterion (classical CS) or in a probabilistic manner using Bayesian approaches [4, 5]. These two approaches are investigated in this paper.

The method we have recently proposed for compressing ultrasound images consists of spatially sampling the image via different acquisition masks and then reconstructing the 2D Fourier transform (FT) of the decimated image [3, 7]. Precisely, in presence of an additive measurement noise, the image can be reconstructed by the following optimization problem

$$\arg\min_{\mathbf{x}} \|\mathbf{y} - \mathbf{T}\mathbf{x}\|_2 + \lambda \|\mathbf{x}\|_1 \tag{2}$$

where $\mathbf{y}$ represents the random spatial samples, $\mathbf{x}$ is the 2D FT of the radiofrequency ultrasound image $\mathbf{m} \in \mathbb{R}^N$ ($\mathbf{x} = \mathbf{F}\mathbf{m}$), $\|.\|_1$ and $\|.\|_2$ are the ℓ_1 and ℓ_2 norms, $\mathbf{T} = \boldsymbol{\Psi}\mathbf{F}^{-1}$ is the sampling matrix, where $\boldsymbol{\Psi}$ indicates the random positions of the spatial samples, $\mathbf{F}$ and $\mathbf{F}^{-1}$ are the direct and inverse 2D FT. In (2), λ is a coefficient weighting the image FT sparsity term (second term) with respect to the data fidelity term (first term). The CS reconstruction conditions depend mainly on the degree of sparsity of $\mathbf{x}$ and on the incoherence between the sparsity basis and the sampling basis. These conditions are valid when $\mathbf{T}$ is a partial Fourier matrix and when the matrix $\boldsymbol{\Psi}$ corresponds to a sampling mask containing 0 outside the principal diagonal and random 0 and 1 in the principal diagonal [3]. Note that the positions of the 1 can be completely random or adapted to UI [3]. Many algorithms are available to solve the problem (2). The optimization routine used in this paper is a non linear conjugate gradient descent algorithm, adapted to large scale problems [3]. This algorithm requires to adjust the parameter λ very carefully (cross validation techniques will be used in the simulation section for adjusting λ). Even if techniques are available for automatically determining the appropriate value of λ [8], the determination of this parameter is still a tedious and challenging issue for practical applications. This paper proposes an original hierarchical Bayesian approach for compressing ultrasound images which considers the penalization parameter λ as an hyperparameter

that can be estimated jointly with the data. The paper is organized as follows: Section 3 formulates the UI reconstruction problem as a Bayesian compressed sensing approach. A Gibbs sampler allowing data to be generated from the posterior distribution of interest is also presented. Simulation results obtained with synthetic and real data are shown in Section 4. Conclusions are finally reported in Section 5.

3. BAYESIAN COMPRESSED SENSING

3.1. Bayesian model

We propose to formulate the sparse reconstruction problem as an estimation problem resolved in a Bayesian framework. The additive noise $\boldsymbol{\eta}$ in (1) is due to instrumentation errors and to deviations from the sparsity hypothesis about the signal $\mathbf{x}$. Because the US image can be complex, we assume that this additive noise is Gaussian complex with a zero mean and unknown variance σ^2. The associated likelihood is

$$p\left(\mathbf{y}|\mathbf{x},\sigma^2\right) = \left(\pi\sigma^2\right)^{-N} \exp\left(-\frac{1}{\sigma^2} \parallel \mathbf{y} - \mathbf{T}\mathbf{x} \parallel_2^2\right)$$

where N is the number of image pixels.

The originality of this paper lies in the consideration of appropriate priors for the unknown parameters $\mathbf{x}$ and σ^2 for UI reconstruction. These priors exploit the Gaussian properties of ultrasound images [9] and the image sparsity in the frequency domain. Precisely, in order to favor the sparsity of the image $\mathbf{x}$ (in our case, $\mathbf{x}$ is the 2D FT of the ultrasound image), each pixel of the image x_i is assigned a prior defined as a mixture of a centered complex normal distribution $\mathcal{CN}\left(0,\sigma_x^2\right)$ and a mass at the origin

$$p(x_i|\sigma_x^2,w) = (1-w)\delta(|x_i|) + \left(\frac{w}{\pi\sigma_x^2}\right)\exp\left(-\frac{|x_i|^2}{\sigma_x^2}\right) \quad (3)$$

where the hyperparameter w is the prior probability of having a non-zero pixel in the image. Note that a similar distribution has already been proposed in [4] for sparse real signal reconstruction. However, the prior proposed in this paper differs from the one developed in [4] since 1) it is defined for complex vectors $\mathbf{x}$ and 2) the continuous density considered in (3) is complex Gaussian whereas it was real exponential in [4]. The Bayesian model is complemented by a classical Jeffreys prior for the noise variance

$$f(\sigma^2) \propto \frac{1}{\sigma^2}.$$

The quality of the reconstruction is partly governed by the hyperparameters w and σ_x^2 involved in the prior (3). In particular, the hyperparameter w is the prior probability of having a non-zero pixel in the image which tunes the sparsity level of the solution $\mathbf{x}$ of the UI reconstruction problem. Thus the choice of the hyperparameters w and σ_x^2 deserves a specific attention. The hierarchical Bayesian reconstruction strategy introduced in this paper proposes to estimate these hyperparameters jointly with the unknown image $\mathbf{x}$ and the noise variance σ^2 from the data using an unsupervised framework. More precisely, appropriate prior distributions are chosen for the hyperparameters w and σ_x^2 that are included within the Bayesian model in a second level of hierarchy. These so-called *hyper-priors* are defined below. Since there is no information about the probability of having a non-zero pixel in the image, w is assigned a uniform distribution on the interval $(0,1)$ denoted as $w \sim \mathcal{U}(0,1)$. The hyperparameter σ_x^2 is assigned a conjugate inverse-gamma distribution with parameters α_0 and α_1 denoted as $\sigma_x^2 \sim \mathcal{IG}(\alpha_0,\alpha_1)$. Hyperparameters α_0 and α_1 are fixed to constant values ensuring the resulting inverse-gamma distribution is non-informative. However, it is important to mention here that we have observed in our experiments that the choice of these hyperparameters is less critical than the direct choice of λ in (2).

The image to be reconstructed is then estimated from its posterior $p(\mathbf{x}|\mathbf{y})$, computed with the following hierarchical Bayesian structure

$$p(\mathbf{x}|\mathbf{y}) \propto \int p\left(\mathbf{y}|\mathbf{x},\sigma^2\right) p(\mathbf{x}|\boldsymbol{\Phi}_x)p(\sigma^2)p(\boldsymbol{\Phi}_x)d\sigma^2 d\boldsymbol{\Phi}_x \quad (4)$$

where $\boldsymbol{\Phi}_x = \left\{w,\sigma_x^2\right\}$, $p(\mathbf{x}|\boldsymbol{\Phi}_x) = \prod_i p(x_i|\boldsymbol{\Phi}_x)$ and $p(\boldsymbol{\Phi}_x) = p(w)p(\sigma_x^2)$ (note that all parameters and hyperparameters are assumed to be independent a priori). Unfortunately, the Bayesian estimators such as the maximum *a posteriori* (MAP) or the mean *a posteriori* estimator relative to the posterior $p(\mathbf{x}|\mathbf{y})$ defined in (4) are difficult to obtain explicitly. Thus, we propose to use a Markov chain Monte Carlo (MCMC) method (known as the Gibbs sampler) for generating vectors that are asymptotically distributed according to the joint posterior distribution $f\left(\mathbf{x},\sigma^2,w,\sigma_x^2|\mathbf{y}\right)$. These generated vectors will be denoted as $\left\{x^{(t)},\sigma^{2(t)},w^{(t)},\sigma_x^{2(t)}\right\}_{t=1,\ldots,N_{MC}}$.

3.2. Gibbs sampler

To generate samples asymptotically distributed according to (4), we propose to use a Gibbs sampler that consists of iteratively sampling according to the conditional distributions associated with the joint posterior $f\left(\mathbf{x},\sigma^2,w,\sigma_x^2|\mathbf{y}\right)$. The successive steps of the Gibbs sampler are summarized below.

3.2.1. Sampling according to $f\left(\mathbf{x}|\sigma^2,w,\sigma_x^2,\mathbf{y}\right)$

The conditional distribution of each pixel x_i given the others $\mathbf{x}_{\setminus i}$ ($\mathbf{x}_{\setminus i}$ denotes the vector $\mathbf{x}$ whose ith element has been removed) is

$$f\left(x_i|\mathbf{x}_{\setminus i},\sigma^2,w,\sigma_x^2,\mathbf{y}\right) = (1-w_i)\delta(|x_i|) + \left(\frac{w_i}{\pi\eta_i^2}\right)\exp\left(-\frac{|x_i-\mu_i|^2}{\eta_i^2}\right) \quad (5)$$

with

$$\begin{cases} \eta_i^2 = \left(\frac{1}{\sigma_x^2} + \frac{\|\mathbf{t}_i\|^2}{\sigma^2}\right)^{-1} \\ \mu_i = \mathbf{t}_i^H \mathbf{e}_i \frac{\eta_i^2}{\sigma^2} \\ w_i = \frac{\tilde{w}_i}{\tilde{w}_i+(1-w)} \end{cases} \text{ and } \begin{cases} \tilde{w}_i = \frac{w\eta_i^2}{\sigma_x^2}\exp\left(\frac{|\mu_i^2|}{\eta_i^2}\right) \\ \mathbf{e}_i = \mathbf{y} - \sum_{j\neq i} x_i \mathbf{t}_i \end{cases}$$

where $\mathbf{t}_i$ is the ith column of $\mathbf{T}$. Consequently, the conditional distribution of x_i is a Bernoulli-Gaussian distribution. Sampling according to $f\left(\mathbf{x}|\sigma^2,w,\sigma_x^2,\mathbf{y}\right)$ is then conducted by generating N distributions $f\left(x_i|\mathbf{x}_{\setminus i},\sigma^2,w,\sigma_x^2,\mathbf{y}\right)$ for $i=1,...,N$.

3.2.2. Sampling according to $f\left(\sigma^2|\mathbf{x},w,\sigma_x^2,\mathbf{y}\right)$

Straightforward computations show that the conditional distribution of the noise variance is the following inverse-Gamma distribution

$$\sigma^2|\mathbf{x},\mathbf{y} \sim \mathcal{IG}\left(M,\|\mathbf{y}-\mathbf{T}\mathbf{x}\|^2\right). \quad (6)$$

3.2.3. Sampling according to $f\left(w|\mathbf{x},\sigma^2,\sigma_x^2,\mathbf{y}\right)$

The conditional distribution of the hyperparameter w is the following beta distribution

$$w|\mathbf{x} \sim \mathcal{B}\left(n_1+1, N-n_1+1\right) \tag{7}$$

with $n_1 = \|\mathbf{x}\|_0$ ($\|\mathbf{x}\|_0$ is the number of non-zero pixels in $\mathbf{x}$).

3.2.4. Sampling according to $f\left(\sigma_x^2|\mathbf{x},\sigma^2,w,\mathbf{y}\right)$

The conditional distribution of the hyperparameter σ_x^2 (a priori variance for non zero pixels) is

$$\sigma_x^2|\mathbf{x} \sim \mathcal{IG}\left(n_1+\alpha_0, \|\mathbf{x}\|^2+\alpha_1\right). \tag{8}$$

4. RESULTS

The reconstruction of a synthetic ultrasound image has been first investigated using the minimization of (2) and the Bayesian approach described in Section 3. The image is a simulated radiofrequency (RF) image of size 128×128 pixels obtained from the Field II program [10] and an *in vivo* human thyroid gland image. The synthetic image represents an homogeneous field crossed by a vessel containing no scatter depicted in Fig. 1(a). A random decimation of this synthetic image has been conducted using a decimation factor of 50%, placing us in a sampling framework that does not obey the Nyquist criterion. The real part of the resulted decimated image is shown in Fig. 1(b). The reconstructed real parts of the images obtained with the minimization of (2) and the proposed Bayesian approach are shown in Fig. 1(c) and 1(d) respectively. It is important to mention here that the parameter λ in (2) was adjusted empirically to give the best reconstruction. The number of iterations of the conjugate gradient algorithm used to solve (2) was set to 200, which was large enough to ensure the convergence in all experiments. The NRMSEs (root mean squared error divided by the root square of the ℓ_2 norm of the original image) are similar for these two images ($E = 0.12$ for the usual CS method and $E = 0.10$ for the proposed Bayesian method). The part of the image corresponding to the inside of the vessel (black area in the original image) results in the worst reconstruction in both cases: it corresponds to a region with a few number of scatters therefore yielding a weak signal.

The reconstruction of an RF line is shown in Fig. 2 for each method. Observe that the signals are well restored. Even if the reconstructions obtained by the two methods have similar errors, the Bayesian approach allows a better estimation of the image statistics as shown in Fig. 3. Indeed, the histogram of the 2D FT of the original image shown in Fig. 3(a) is closer to the one obtained with the image estimated using the Bayesian approach, which is an interesting property.

As mentioned before, the Bayesian algorithm allows the probability of having a zero pixel to be estimated (in addition to image reconstruction). Fig. 4 shows the histogram of the samples $w^{(t)}$ generated using the proposed simulation method. The corresponding minimum mean squared error (MMSE) estimator is $\widehat{w}_{\text{MMSE}} = 0.55$ which is close to the true value $w = 0.50$. The samples generated by the proposed Gibbs sampler can also be used to estimate the unknown parameters $\sigma_x^{2(t)}$ and $\sigma^{2(t)}$. Figures 5 and 6 show the histograms of the samples $\sigma_x^{2(t)}$ and $\sigma^{2(t)}$ respectively. The MMSE estimators are $\widehat{\sigma^2}_{\text{MMSE}} = 1.75 \times 10^{-13}$ and $\widehat{\sigma_x^2}_{\text{MMSE}} = 0.46$.
Similar results obtained for *in vivo* images of a human thyroid gland are provided in Fig. 7. The right lobe thyroid gland image was acquired with a clinical scanner (Sonoline Elegra, Siemens Medical Systems, Issaquah, WA, USA), whose sampling frequency was adjusted to 40 MHz. The obtained results are very promising.

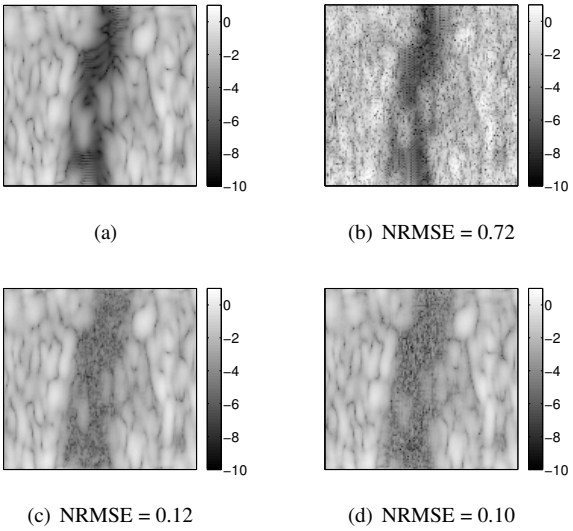

(a) (b) NRMSE = 0.72

(c) NRMSE = 0.12 (d) NRMSE = 0.10

Fig. 1. (a) Real part of an original synthetic image of a blood vessel, (b) 50% of the spatial samples used for reconstruction, (c) real part of the reconstructed image using the minimization of (2) and (d) real part of the reconstructed image by Bayesian approach. The dashed line corresponds to the RF signal plotted in Fig. 2

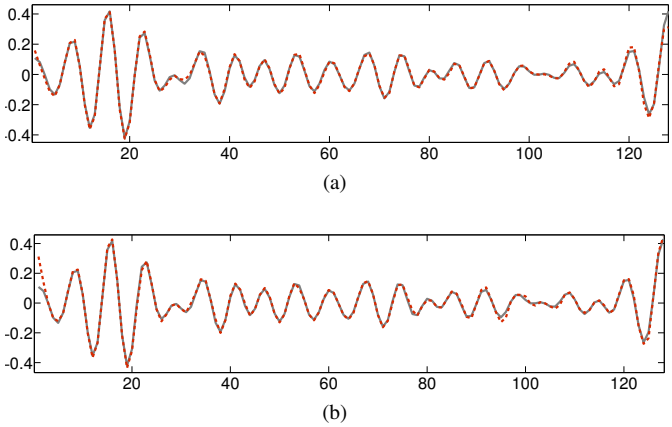

(a)

(b)

Fig. 2. Results of reconstruction (dashed red line) of an original RF line (grey continuous line) by (a) minimization of (2) and (b) Bayesian approach (50% of missing spatial samples). The RF line corresponds to the vertical dashed line depicted in Fig. 1(a).

5. CONCLUSION

This paper presents a Bayesian reconstruction method for ultrasound images. The main advantage of the proposed Bayesian approach compared to a classical ℓ_1 minimization method is that there is no need to adjust a regularization parameter (such as λ defined in (2)). In addition, the algorithm developed in this work allows the degree of sparsity of the image in the frequency domain to be estimated. This sparsity measure can be used to design appropriate

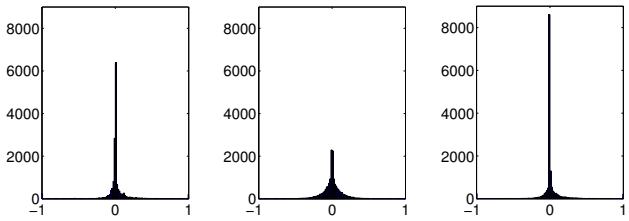

Fig. 3. Histograms of $\Re(x)$ (real part of the ultrasound image FT) for the (a) original image, (b) reconstructed image by minimization of (2) and (c) reconstructed image by the proposed Bayesian approach (50% missing spatial samples).

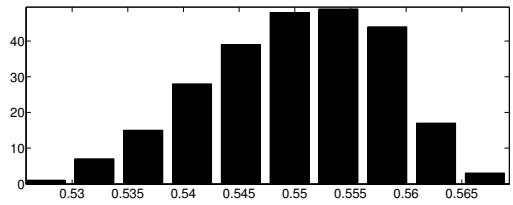

Fig. 4. Histogram of the samples $w^{(t)}$ for $t = 250, ..., 500$.

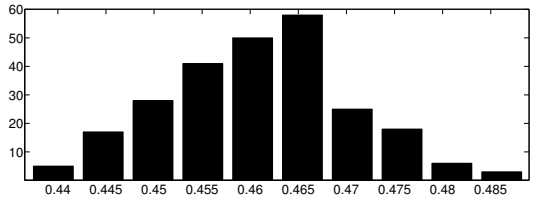

Fig. 5. Histogram of the samples $\sigma_x^{2(t)}$ for $t = 250, ..., 500$.

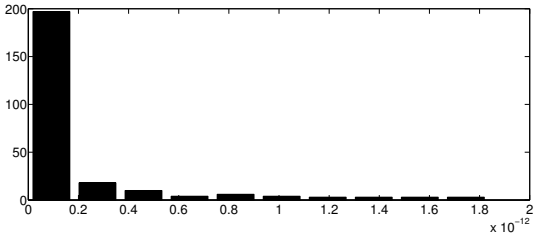

Fig. 6. Histogram of the samples $\sigma^{2(t)}$ for $t = 250, ..., 500$.

subsampling strategies for ultrasound images. Future works include the study of a GP/GPU implementation of the proposed algorithm in order to reduce the current execution time. Including some characteristic pattern of the image in the frequency domain is also under investigation.

6. REFERENCES

[1] E. J. Candes, J. Romberg, and T. Tao, "Robust uncertainty principles: exact signal reconstruction from highly incomplete frequency information," *IEEE Trans. Inf. Theory*, vol. 52, no. 2, pp. 489–509, Jan. 2006.

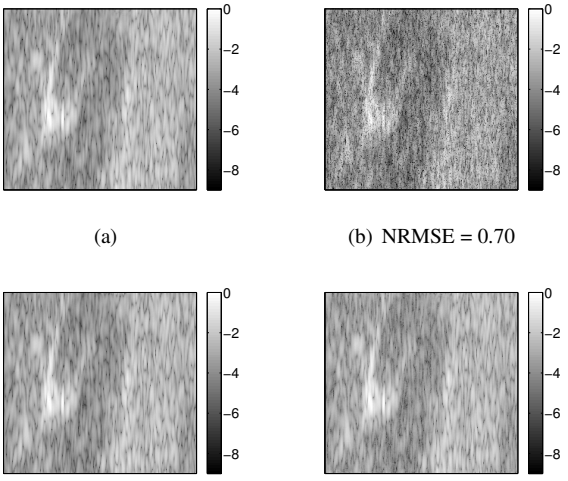

Fig. 7. (a) Real part of an original *in vivo* image of a human thyroid gland, (b) 50% of spatial samples used for reconstruction, (c) real part of reconstructed image by minimization of (2) and (d) real part of the reconstructed image by the Bayesian approach.

[2] J. Provost and F. Lesage, "The application of compressed sensing for photo-acoustic tomography," *IEEE Trans. Medical Imaging*, vol. 28, no. 4, pp. 585–594, April 2009.

[3] C. Quinsac, A. Basarab, J.-M. Gregoire, and D. Kouame, "3D compressed sensing ultrasound imaging," in *Proc. IEEE Int. Ultrason. Symp. (IUS), San Diego, U.S.A.*, Oct. 2010.

[4] N. Dobigeon, A. O. Hero, and J.-Y. Tourneret, "Hierarchical Bayesian sparse image reconstruction with application to MRFM," *IEEE Trans. Image Processing*, vol. 18, no. 9, pp. 2059–2070, Sept. 2009.

[5] S. Ji, Y. Xue, and L. Carin, "Bayesian compressive sensing," *IEEE Trans. Signal Process.*, vol. 56, no. 6, pp. 2346–2356, 2008.

[6] B. Raju and M. Srinivasan, "Statistics of envelope of high-frequency ultrasonic backscatter from human skin in vivo," *IEEE Trans. on Ultrasonics, Ferroelectrics and Frequency Control*, vol. 49, no. 7, pp. 871 –882, July 2002.

[7] C. Quinsac, A. Basarab, J.-M. Girault, and D. Kouame, "Compressed sensing of ultrasound images: Sampling of spatial and frequency domains," in *Proc. IEEE Workshop on Signal Process. Syst. (SIPS)*, Oct. 2010, pp. 231–236.

[8] E. Candes, M. Wakin, and S. Boyd, "Enhancing sparsity by reweighted l1 minimization," *J. Fourier Anal. Appl.*, vol. 14, no. 5, pp. 877–905, 2008.

[9] R. F. Wagner, M. F. Insana, and D. G. Brown, "Statistical properties of radio-frequency and envelope-detected signals with applications to medical ultrasound," *J. Opt. Soc. Am. A*, vol. 4, no. 5, pp. 910–922, May 1987.

[10] J. A. Jensen and N. B. Svendsen, "Calculation of pressure fields from arbitrarily shaped, apodized, and excited ultrasound transducers," *IEEE Trans. on Ultrasonics, Ferroelectrics and Frequency Control*, vol. 39, no. 2, pp. 262–267, March 1992.